

Trojan-Horse Nanotube On-Command Intracellular Drug Delivery

*Chia-Hsuan Wu, ^{†,∇} Cong Cao, ^{‡,∇}, Jin Ho Kim, [†] Chih-Hsun Hsu, [†] Wayne D. Bowen, [‡]
Harold J. Wanebo, [§] Jimmy Xu, ^{†,||,*} and John Marshall, ^{‡,*}*

[†]School of Engineering and [‡]Department of Molecular Pharmacology, Physiology and
Biotechnology, Brown University, Providence, RI 02912, United State

[§]Division of Surgical Oncology, Landmark Medical Center, Woonsocket, RI 02895,
United State

^{||}World Class University program, Seoul National University, Seoul 151-742, Korea

*To whom correspondence should be addressed.

E-mail: J. X. (Jimmy_Xu@Brown.Edu) or J. M. (John_Marshall@Brown.Edu).

[∇]These authors contributed equally to this work.

SUPPLEMENTARY INFORMATION

Materials and Methods

Taxol/C6-ceramide loading into CNT arrays. The CNT array is fabricated on an anodized aluminum oxide (AAO) template using a CVD process, and opened on both ends by chemical treatment.¹ The drug loading was performed by applying the mixture of Taxol/C6-ceramide and gelatin (0.2 g/mL, Sigma-Aldrich) solution on top of a vertically aligned nanotube array with a vacuum suction at the bottom. After loading, the individual CNTs were released from the alumina template by 0.1 M NaOH treatment. The solution was then filtered through filter paper (Millipore, pore size 50nm) to remove excess NaOH, and washed thoroughly with deionized water. The released CNTs were first treated with diluted nitric acid to reduce their length to 200-1000 nm. Afterwards, CNTs were further sonicated with amine-terminated phospholipid-polyethylene glycol [PL-PEG, 0.1-1 mg/mL of DSPE-PEG (2000) Amine, Avanti Polar Lipids Inc.] for 1h.² The mixture was then filtered through filter paper and washed thoroughly with water. The as-synthesized Trojan-Horse CNTs with payload in solution form was stored in the buffer solution for up to one week with the drug remaining intact.

TexasRed labeled Trojan-Horse nanotubes. The pH of the CNT solution that was non-covalently functionalized with amine-terminated polyethylene glycol phospholipids (PL-PEG-NH₂) was adjusted to 8.5 with sodium tetraborate decahydrate buffer. Texas Red-X succinimidyl ester (Invitrogen, NY) dissolved in dimethylsulfoxide was mixed with the CNT solutions at room temperature overnight. Following the reaction, the mixture

solution was filtered (Millipore, pore size 50 nm) to remove unincorporated dye, and washed thoroughly with deionized water.

Antibodies and reagents. C6-ceramide was obtained from Avanti Polar Lipids Inc. Taxol was supplied by RI Landmark Medical Center. p-Akt (Ser 473), Akt1/2 and cleaved-caspase 3 primary antibodies were obtained from Cell Signaling Tech (Beverly, MA). Mouse mono-clonal antibody against β -actin was obtained from Sigma (St Louis, MO).

Cell apoptosis assay (Histone DNA-ELISA). The Cell Apoptosis ELISA Detection Kit (Roche, Palo Alto, CA) was used to detect pancreatic cancer cell apoptosis after indicated treatments according to the manufacturer's protocol. Briefly, the cytoplasmic histone/DNA fragments from treated cells were extracted and bound to immobilized anti-histone antibody. Subsequently, the peroxidase-conjugated anti-DNA antibody was then added for the detection of immobilized histone/DNA fragments. After addition of substrate for peroxidase, the spectrophotometric absorbance of the samples was determined by using a Perkin Elmer 1420 multilabel counter at 405 nM.

Cell culture, viability assay. Human pancreatic cancer lines PANC-1, MIA PaCa-2 (MIA) and L3.6 cells culture, cell viability assay (MTT dye assay) were performed 48 hours after treatment as previously described³.

Western blot analysis. L3.6 cells treated with the appropriate stimuli were lysed with lysis buffer (200 mM NaCl (pH 7.4), 1% Triton X-100, 10% glycerol, 0.3 mM EDTA, 0.2 mM Na_3VO_4 , and protease inhibitor cocktail (Roche Diagnostics, Indianapolis, IN). Aliquots of 40 μg of protein from each treatment were separated by 10% SDS–polyacrylamide gel electrophoresis (SDS-PAGE) and transferred onto a polyvinylidene

difluoride (PVDF) membrane (Millipore, Bedford, MA). After blocking with 10% instant nonfat dry milk for 1 hour, membranes were incubated with specific antibodies overnight at 4°C followed by incubation with secondary antibodies (HRP-conjugated anti-rabbit or anti-mouse IgG at the appropriate dilutions) for 1 hour at room temperature. Antibody binding was detected with the enhanced chemiluminescence (ECL) detection system (Amersham Biosciences, Piscataway, NJ).

Statistics. The values in the figures are expressed as the means \pm standard deviation (SD). A two tailed student's t-test was used for measuring statistical significance of quantitative MTT OD results. Results were deemed significant where * $p < 0.05$

Experimental and control data on the cellular uptake of CNT.

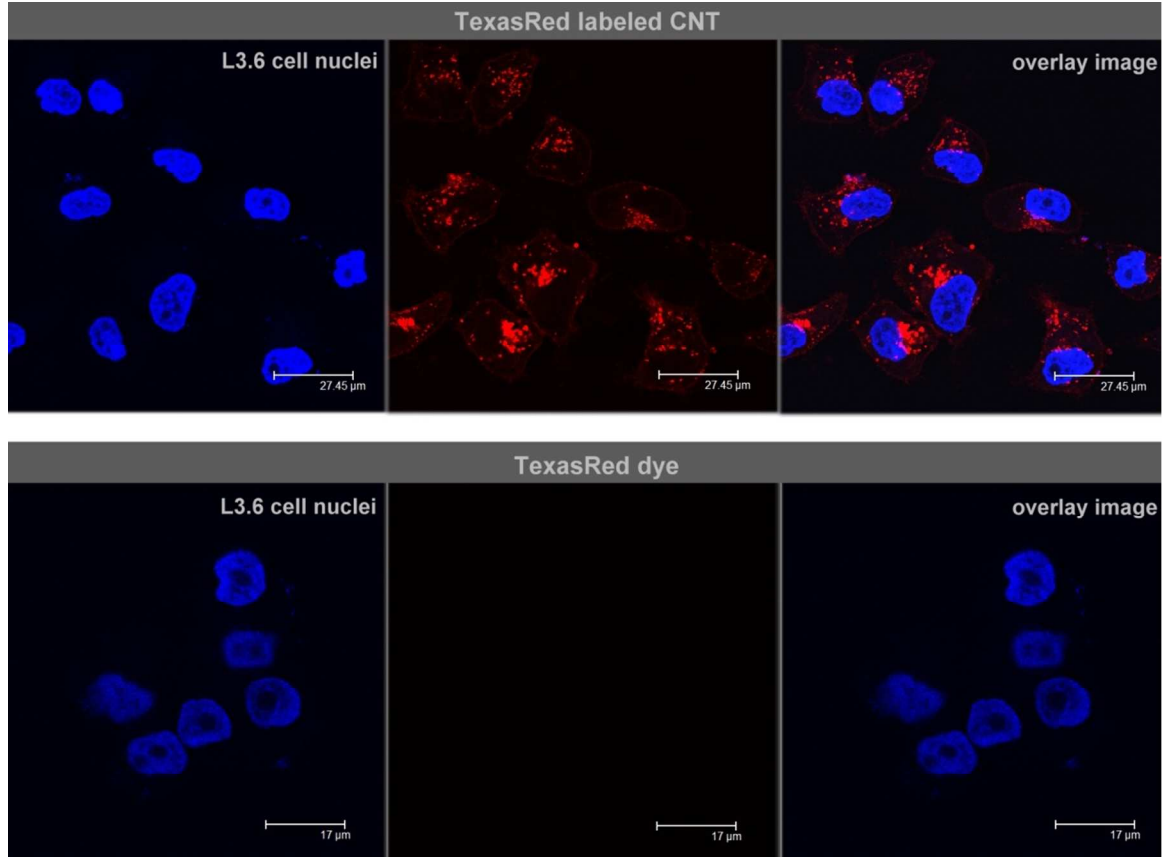


Figure S1. Confocal fluorescence images in plan-view of L3.6 pancreatic cancer cells taken after overnight incubation with Texas Red-labeled Trojan-Horse nanotubes and with Texas Red dye respectively. L3.6 cell nuclei were stained in blue with Hoechst 33342 (left), Texas Red dye is shown in red (center) and overlay images of blue and red (right).

Mechanism of Taxol-induced cancer cell death.

Taxol (Paclitaxel) binds to the β -tubulin subunit to enhance polymerization and inhibit depolymerization of microtubules, resulting in cell cycle arrest and eventually apoptosis.⁴ However, recent studies demonstrate that Taxol initiates cell death and apoptosis through multiple mechanisms, of which, checkpoint of mitotic spindle assembly⁵, aberrant activation of cyclin-dependent kinases⁵, and the c-Jun N-terminal kinase/stress-activated protein kinase (JNK/SAPK)⁶ are the major signaling mediators⁴. As shown in Figure S2, we performed a cell viability time course study that demonstrated that 48h was required to observe significant cell death by encapsulated Taxol and C6-ceramide. As shown in Figure S3, we found that a lower dose of encapsulated Taxol and C6-ceramide significantly produced (30%) less cell death. Exogenous C6 ceramide has been shown to sensitize multiple cancer cell lines to chemotherapeutic-induced apoptosis by promoting AMPK activation and mTORC1 inhibition.⁷

Time course study on cell viability after the treatment with CNT encapsulated Taxol /C6-ceramide.

In vitro studies with the encapsulated drugs within CNT were performed, and a plot of cell viability versus time (6h, 12h, 24h, and 48h) after a.c. magnetic field stimulation is shown below.

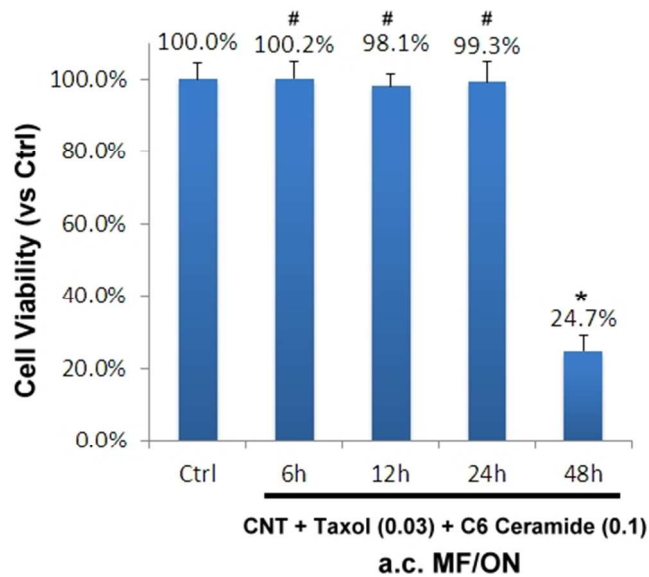


Figure S2. Time course study on cell viability after the treatment with CNT containing the drugs [Taxol (0.03 μ g/ml) + C6-Ceramide (0.1 μ g/ml)]. The CNT-exposed L3.6 cells were subjected to the a.c. magnetic field, and cultured for the indicated time points (6h, 12h, 24h and 48h). The number of viable cells in 10 random microscope views was counted for each condition, and normalized to the control group (no a.c. magnetic stimulation). Results demonstrate that no significant cell death was observed less than 48h after a.c. magnetic field stimulation. (* p <0.05 vs. Ctrl, # p >0.05 vs. Ctrl)

Cell viability versus CNT-Taxol-C6 concentration.

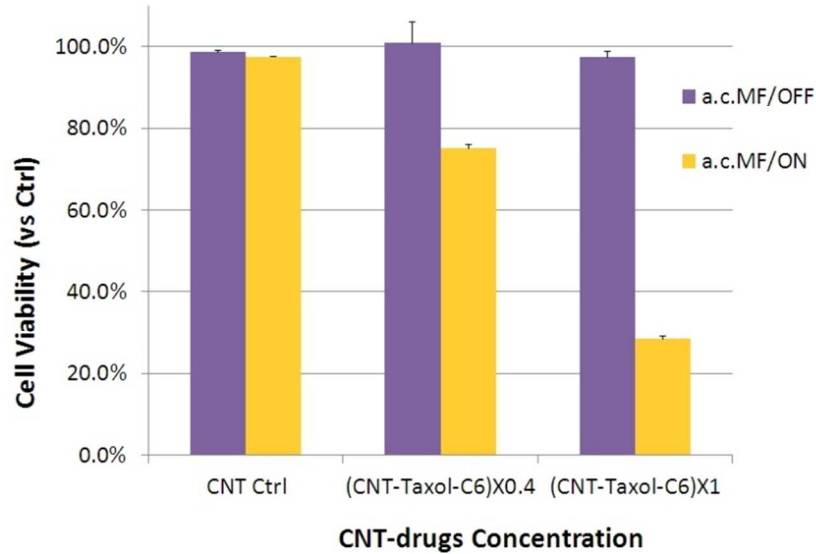


Figure S3. Plot of cell viability versus CNT-drugs concentration. The cells were exposed to the CNT with drugs (Taxol/C-6 ceramide) encapsulated for 48 hours, after which a cell viability MTT assay was performed. The CNT-Taxol-C6) x 1 drug concentration [Taxol (0.03 μ g/ml) + C6-Ceramide (0.1 μ g/ml)] was effective, resulting in over 70% cell death. Reducing the drug concentration to 0.4 x of (CNT-Taxol-C6) substantially reduced cell death to about 30%. The results show that the encapsulated concentrations of [Taxol (0.03 μ g/ml) and C6-Ceramide (0.1 μ g/ml)] are optimal for producing cell death.

Induction Heating of Trojan-Horse CNTs.

According to Lenz's law, swirls of currents (called Eddy current) in the conductor will be induced in order to generate an opposed magnetic field when the conductor experiences a change in magnetic field. By exposing the conductor in a time-varying magnetic field (or called a.c. magnetic field), the induced Eddy current give rises to the induction Joule heating. Multi-walled carbon nanotube is intrinsically an electron conductor that makes it an excellent candidate for the on-demand drug delivery vehicle.

Starting with the Maxwell equation form of Faraday's Law, $\nabla \times \mathbf{E} = -\frac{\partial \mathbf{B}}{\partial t}$ describes that the time varying magnetic field (B) creates the electric field (E).

It is known that the penetration depth δ (m), $\delta = \frac{1}{\sqrt{\pi f \mu \sigma}}$ is much larger (~millimeter) than the physical dimension of CNTs (~200 nanometer)⁸. Where f is frequency of alternating magnetic field, μ denotes as magnetic permeability and σ is the electrical conductivity (S/m). Therefore, we can consider the case is under quasi-statics condition where the electromagnetic wave fully penetrates the CNTs.

Under such condition, one can estimate the power generated by the induced Eddy current of a nanotube. Note that we simplify the case by assuming there is not magnetization of the CNTs. Therefore, the current density

$$\mathbf{J} = \sigma \mathbf{E} = i\sigma \omega \mathbf{B}, \dots \dots \dots \text{Eq.(S.1)}$$

As described earlier in Eq (S.1), $\mathbf{J} = \sigma \mathbf{E} \Rightarrow \mathbf{I} = A\sigma \omega \mathbf{B}$

We then derive the power generated from the induced Eddy current below:

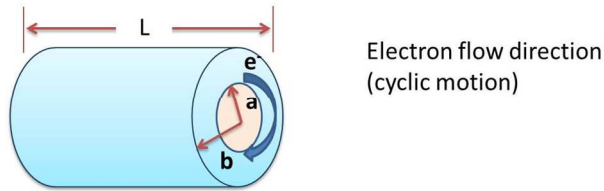
$$\mathbf{P} = I^2 R = I^2 \cdot \rho \cdot \frac{l}{A} \dots \dots \dots \text{Eq.(S.2)}$$

Where l is the length of CNT, A is CNT surface area, ρ is the resistivity of CNT and R is the resistance of CNT.

By substituting Eq.(S.2) into Eq. (S.1), we now get the expression of the induced power of individual CNT.

$$\mathbf{P} = A\sigma^2 \cdot \omega^2 \cdot B^2 \cdot l \cdot \rho = \frac{\omega^2 B^2}{\rho} \cdot (A \cdot l) \dots \dots \dots \text{Eq.(S.3)}$$

Now, we would have to estimate the resistance of the multiwalled CNTs. Assume the electrons flow in a cyclic motion like the graph below:



Where

$$\begin{cases} l = \left(\frac{R_{out} + R_{in}}{2} \right) \cdot 2\pi \\ A = (R_{out} - R_{in}) \cdot L \end{cases}$$

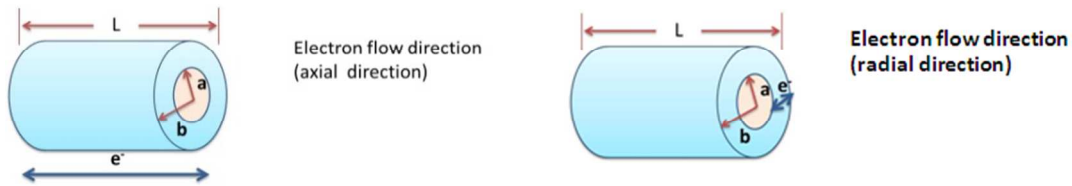
Applying the above relationship to Eq. (S.3), we get the the expression

$$\begin{aligned} \mathbf{P} &= \frac{\omega^2 B^2}{\rho} \cdot (Al) = \frac{\omega^2 B^2}{\rho} [L \cdot (R_{out} - R_{in})] \cdot \left[2\pi \cdot \left(\frac{R_{out} + R_{in}}{2} \right) \right] \\ &= \frac{\pi L \omega^2 B^2}{\rho} (R_{out}^2 - R_{in}^2) \end{aligned}$$

The Joule heating power P (W/kg) generated by induced Eddy current is given by

$$P \propto B^2 \omega^2 (R_{out}^2 - R_{in}^2) L / \rho$$

Where B is peak flux density magnetic field (T), L is the length of nanotube (m), ω is the frequency (Hz), ρ denotes the resistivity of nanotube (Ωm), R_b and R_a are the outer and inner radius of nanotube, respectively (m).



Here we only include one calculation with electron flow in cyclic motion. We also have estimations with axial direction and radial direction. The results from three cases are all the same.

The extent of heating generated in each nanotube is controlled by the applied magnetic field strength, frequency, and by the tube's resistivity and physical dimension, the former two parameters could be controlled via the application of induction source power, whereas the latter two are controllable by our fabrication process.

REFERENCES

- (1) Li, J.; Papadopoulos, C.; Xu, J.; Moskovits, M. *Appl. Phys. Lett.* **1999**, 75 (3), 367-369.
- (2) Kam, N.W.; Liu, Z.; Dai, H. *J. Am. Chem. Soc.* **2005**, 127 (36), 12492-12493.

- (3) Cao, C.; Huang, X.; Han, Y.; Wan, Y.; Birnbaumer, L.; Feng, G. S.; Marshall, J.; Jiang, M.; Chu, W. M. *Science signaling* **2009**, 2, (68), ra17.
- (4) Wang, T. H.; Wang, H. S.; Soong, Y. K. *Cancer* **2000**, 88, (11), 2619-2628.
- (5) Shu, C. H.; Yang, W. K.; Shih, Y. L.; Kuo, M. L.; Huang, T. S. *Apoptosis* **1997**, 2, (5), 463-470.
- (6) Lee, L. F.; Li, G.; Templeton, D. J.; Ting, J. P. *J. Biol. Chem.* **1998**, 273, (43), 28253-28260.
- (7) Ji, C.; Yang, B.; Yang, Y.-L.; He, S.-H.; Miao, D.-S.; He, L.; Bi, Z.-G. *Oncogene* **2010**, 29, (50), 6557-6568.
- (8) Vagner, I.D.; Lembrikov, B.I.; Wyder P.R. *Electrodynamics of magnetoactive media*; Springer-Verlag Berlin Heidelberg: New York, **2004**.